Multiobjective Heuristic Approaches to Seismic Design of Steel Frames with Standard Sections[1]

M. Ohsaki

Department of Architecture and Architectural Engineering,
Kyoto University Kyotodaigaku-Katsura, Nishikyo, Kyoto 615-8540, Japan

T. Kinoshita

Department of Architecture and Architectural Engineering,
Kyoto University Kyotodaigaku-Katsura, Nishikyo, Kyoto 615-8540, Japan

P. Pan

Department of Civil Engineering, Tsinghua University,
Beijing 100084, P.R. China

Abstract

Seismic design problem of a steel moment-resisting frame is formulated as a multiobjective programming problem. The total structural (material) volume and the plastic dissipated energy at the collapse state against severe seismic motions are considered as performance measures. Geometrically nonlinear inelastic time-history analysis is carried out against recorded ground motions that are incrementally scaled to reach the predefined collapse state. The frame members are chosen from the lists of the available standard sections. Simulated Annealing (SA) and Tabu Search (TS), which are categorized as single-point-search heuristics, are applied to the multiobjective optimization problem. It is shown in the numerical examples that the frames that collapse with uniform interstory drift ratios against various levels of ground motions can be obtained as a set of Pareto optimal solutions.

Keywords Seismic design; Multiobjective programming; Plastic dissipated energy; Steel frame; Simulated annealing; Tabu search

1 Introduction

In the framework of performance-based design of steel moment-resisting frames, several performance states such as immediate occupancy and collapse prevention should be investigated against seismic motions with specified levels. In this paper, we consider the collapse state defined so that the roof displacement reaches the specified value [1, 2, 3]. In order to evaluate the loading capacity at collapse state of a steel frame, the seismic excitation is usually modeled as equivalent static loads, for which the responses are found by the incremental procedure called static pushover analysis. However, it is preferable to evaluate the seismic responses by time-history analysis, if the dynamic effects are to be fully incorporated.

The criteria for the seismic design are generally classified as

[1]This paper has appeared in: Earthquake Engng. Struct. Dyn., Vol. 36(11), pp. 1481–1495, 2007.

- The story displacements and the local deformations such as the strains at the connections should not exceed the given upper bound against equivalent static loads or ground motions with specified level.
- The load level should be large enough at the predefined collapse state, and the collapse mechanism should not consist of unfavorable local deformation.

In the approach based on the first criterion, which is a traditional code-based approach of seismic design, we can find the safety margin of the structure in view of deformation at the specified load level, but the margin of the load level to collapse is unknown [4]. On the contrary, in the approach based on the second criterion, which is a standard approach of performance-based design, the ultimate load resisting capacity is evaluated and the local behavior at collapse is investigated. Several other performance states such as immediate occupancy are to be investigated for evaluating the structural performances against moderately small earthquakes [5].

In this paper, we adopt the second criterion; i.e., the level of the ground motion leading to the collapse state of a moment-resisting frame is evaluated by an incremental dynamic analysis. In the inelastic design of frames, the collapse mechanism with widely distributed plastic hinges at beam ends are preferred. Such a design can be obtained by maximizing the dissipated energy for specified roof displacement at collapse state. Another importance in consideration of the dissipated energy is that the response of the structures can be approximately evaluated by the balance of input and dissipated energies [6]. On the other hand, the amount of the energy to be dissipated under specified deformation is strongly related to the total structural (material) volume. Hence, the structural volume controls the level of seismic motion that leads to the collapse state. Therefore, a design with favorable collapse mechanism with uniform interstory drift ratios can be obtained by simultaneously minimizing the total volume and maximizing the dissipated energy.

Since the structural performances need to be maximized under various design requirements, the seismic design problem is naturally formulated as an optimization problem [4, 7, 8]. If the design variables such as the cross-sectional areas of the members are continuous variables, the optimization problem can be solved by a gradient-based nonlinear programming approach [9]. However, if the cross-sections of the beams and columns of the steel frames are to be chosen from a list or a catalog of the available standard sections [10], the design problem turns out to be a combinatorial optimization problem, for which the global optimal solution is very difficult to obtain.

Recently, owing to the rapid development of computer hardware and software technologies, we can carry out structural analysis many times to obtain optimal solutions. Furthermore, in the practical design process, it may be enough to obtain an approximate optimal design, i.e., the global optimal design need not be obtained. Heuristic approaches (or heuristics for simplicity) have been developed to obtain approximate optimal solutions within reasonable computational cost, although there is no theoretical proof of convergence [11]. The most popular approach is the genetic algorithm [12], which can be categorized as a multipoint search or population-based method that has many solutions at each iterative step called generation. Since computational cost for evaluating the objective and/or constraint functions at each step is relatively large for

structural optimization problems compared with that for mathematically defined toy problems, a multipoint strategy may not be appropriate especially for optimization of a structure with large number of degrees of freedom. Therefore, single-point-search heuristics such as Simulated Annealing (SA) [13] and Tabu Search (or Taboo Search, TS) [14] may have advantage over the multipoint strategies.

In addition to maximizing the energy dissipation capacity, it is also important to reduce the structural volume that approximately represents the cost for the steel. Therefore, in this paper, the design problem is formulated as a MultiObjective Programming (MOP) problem [15, 16]. Pareto optimal solutions are generated for a plane frame by improved multiobjective SA and TS. The responses at the collapse state under seismic motions are computed by time-history analysis considering geometrical and material nonlinearities, where the peak ground velocities of the recorded motions are incrementally scaled to the level leading to the collapse state. The computational performances of the methods and the characteristics of the solutions are discussed by using a 5-story 4-span plane frame.

2 Evaluation of seismic performance

It is important in the seismic design of moment-resisting frames that the local story mechanism should be avoided to ensure the required energy dissipation capacity before reaching the collapse state. Therefore, if the collapse state is defined by deformation level such as the roof displacement, the plastic dissipated energy E_{p} is to be maximized in the same manner as the optimization of elastic structures for maximizing the strain energy for given deformation. On the contrary, if E_{p} is defined as the dissipated energy for the specified seismic level, then E_{p} should be minimized to obtain a design with enough stiffness, which corresponds to the traditional optimization problem of elastic structures for minimizing the strain energy for specified load level. However, minimization of dissipated energy at collapse state leads to unfavorable story collapse mechanism. Therefore, in this paper, we maximize the dissipated energy at the collapse state to ensure the overall collapse mechanism.

The typical three recorded motions; (i) El Centro NS (1940), (ii) Hachinohe NS (1968), and (iii) Taft EW (1952) are used after scaling by the Peak Ground Velocity (PGV). Note that any site-dependent earthquake or design-spectrum-compatible motion can be used. The ground motions can also be scaled by Peak Ground Acceleration (PGA). However, it is well known that the input energy is closely related to PGV, rather than the instantaneous peak of acceleration. Therefore, we use PGV, because the dissipated energy is considered as performance measure of the frame.

Let z denote a representative response quantity such as a story displacement, the plastic dissipated energy, and so on. The maximum response $z^{\max}$ is defined as the maximum absolute value among the responses z^{i}, z^{ii} and z^{iii} for the three motions (i), (ii) and (iii).

The maximum responses are computed by time-history analysis considering both geometrical and material nonlinearities modeled by a generalized plastic hinge considering the interaction between the bending moment and axial force in yield condition.

Since the geometrically nonlinear inelastic responses are not proportional to the magnitude of the input seismic motion, $z^{\max}$ is evaluated by an incremental dynamic analysis [17].

Denote by H and $d^{\max}$ the total height of the frame and the maximum response displacement at the roof level, respectively. The collapse state is defined by

$$d^{\max} = \beta H \tag{1}$$

where β is the specified average interstory drift ratio. The PGV of the ground motion is increased until the collapse condition (1) is satisfied.

The PGV $v_k^{\max}$ of the kth-level ground motion is defined by

$$v_k^{\max} = v_1^{\max} + \Delta v^{\max}(k-1) \tag{2}$$

where $v_1^{\max}$ is the specified PGV for the smallest motion, and $\Delta v^{\max}$ is the increment of the PGV. A value corresponding to the kth-level motion is indicated by subscript $(\ )_k$.

The responses at collapse state are evaluated by the following incremental dynamic analysis with interpolation:

Step 1: Set $v_1^{\max}$ and $\Delta v^{\max}$, and initialize the ground motion level as $k = 1$.

Step 2: Calculate PGV by (2), and carry out time-history analysis to compute the maximum roof displacement $d_k^{\max}$ and the maximum values $z_k^{(i)\max}$ of the preselected responses $z_k^{(i)}$ $(i = 1, \ldots, q)$, where q is the number of response quantities.

Step 3: If $d_k^{\max} < \beta H$, let $k \leftarrow k+1$ and go to Step 2. Otherwise, let $s = k$, and linearly interpolated $z^{\max}$ at collapse between the values for $s-1$ and s as

$$\alpha = \frac{\beta H - d_{s-1}^{\max}}{d_s^{\max} - d_{s-1}^{\max}} \tag{3}$$

$$z^{(i)\max} = (1-\alpha) z_{s-1}^{(i)\max} + \alpha z_s^{(i)\max}, \quad (i = 1, \ldots, q) \tag{4}$$

If the frame collapse under more than one seismic motions of the same level, the smallest values of the dissipated energy should be taken as $E_{\mathrm{p}}^{\max}$ to be maximized, because it represents the worst-case scenario. However, $E_{\mathrm{p}}^{\max}$ is defined, in a similar manner as other response quantities, as the maximum value of E_{p} among the three ground motions. The maximum value $E_{\mathrm{p}}^{\max}$ at the final sth-level generally corresponds to the ground motion leading to collapse state, and the frame does not collapse under the other two seismic motions.

3 Seismic design problem

Suppose a list of the available standard sections is given for each member of a moment-resisting steel frame. The cross-sectional property of the member i is defined by the

cross-sectional area A^i, the second moment of inertia I^i and the plastic section modulus $Z^i_{\rm p}$, which are to be selected from the list M^i as

$$M^i = \{(A^i_1, I^i_1, Z^i_{\rm p1}), \ldots, (A^i_{r_i}, I^i_{r_i}, Z^i_{{\rm p}r_i})\} \tag{5}$$

where r_i is the number of elements in the list.

The integer variable J_i defines the cross-section of the ith member. Let m denote the number of members. If $J_i = j$ $(i = 1, \ldots, m)$, the jth section $(A^i_j, I^i_j, Z^i_{{\rm p}j})$ in M^i is assigned to the ith member. Hence, the mechanical property of the frame is defined by the vector $\mathbf{J} = \{J_i\}$, which is taken as the integer design variable vector.

The total structural volume to be minimized is denoted by $V(\mathbf{J})$. $E^{\max}_{\rm p}$ is also chosen as the objective function to be maximized. Hence, the multiobjective structural optimization problem is formulated as [18, 16]

$$\begin{aligned} \text{MOP}: \ & \text{minimize} \quad V(\mathbf{J}) \ \text{ and } \ -E^{\max}_{\rm p}(\mathbf{J}) && (6)\\ & \text{subject to} \quad R^{\max}(\mathbf{J}) \le \bar{R}^{\max}, && (7)\\ & \qquad\qquad J_i \in \{1, \ldots, r_i\}, \quad (i = 1, 2, \ldots, m) && (8) \end{aligned}$$

where $R^{\max}$ denotes the maximum interstory drift ratio among all stories corresponding to all the seismic motions for the initial PGV level $v^{\max}_1$. If $R^{\max}$ exceeds the moderately large upper bound $\bar{R}^{\max}$, then the solution is simply rejected and the incremental process is not carried out, because the frame will collapse prematurely exhibiting unfavorable story mechanism. This way, the computational cost for performance evaluation at each step of optimization is reduced.

Let $F_1(\mathbf{J}) = V(\mathbf{J})$ and $F_2(\mathbf{J}) = -E^{\max}_{\rm p}(\mathbf{J})$. For two feasible solutions $\mathbf{J}^1$ and $\mathbf{J}^2$ satisfying the constraints, if $F_i(\mathbf{J}^1) \le F_i(\mathbf{J}^2)$ for $i = 1, 2$ and $F_j(\mathbf{J}^1) < F_j(\mathbf{J}^2)$ for $j = 1$ or 2, then $\mathbf{J}^2$ is said to be dominated by $\mathbf{J}^1$. If there is no solution that dominates $\mathbf{J}^*$, then $\mathbf{J}^*$ is called *nondominated solution*, *noninferior solution*, *compromise solution* or *Pareto optimal solution*, which is called Pareto solutions, for simplicity, in the remainder of this paper. The designer or the decision maker can select a Pareto solution according to his/her preference or to another performance measure, because a Pareto solution is a kind of a compromise solution which cannot improve all the objective functions.

The problem MOP (6)–(8) is classified as a combinatorial multiobjective programming problem, because it has integer variables and multiple objective functions. There are several approaches for obtaining Pareto solutions of a combinatorial multiobjective programming problem. However, a computationally efficient optimization approach is desired for the current problem, because time-history analysis should be carried out several times for evaluation of the objective functions for each intermediate solution in optimization process.

4 Heuristic approaches

The approaches to MOP are classified to *priori-articulation of preference* and *posteriori-articulation of preference* [16]. In the priori-articulation approach, the objective functions are combined or transformed to constraints to formulate a single-objective problem. This approach is suitable for the case where the designer's preference is rather fixed, because the single-objective problem should be modified and solved iteratively if the solution is not preferred by the designer. In the posteriori-articulation approach, on the other hand, a set of Pareto solutions is first generated, and the most preferred solution is selected from the set by the designer. In this paper, we use the posteriori-articulation approach because the preferable values of the total structural volume and the dissipated energy are difficult to be assigned a priori.

Several heuristics have been developed for simultaneously generating a diverse set of Pareto solutions. Among them, we use SA and TS, which are categorized as single-point-search heuristics. SA has been shown to be very effective to the problems with many local optimal solutions, because it allows a move to a non-improving solution. Recently, SA has been extended to MOP [19], and we follow the basic framework in [20]. The following options are introduced to improve the convergence property to the Pareto solutions with enough diversity:

- In the process of generating neighborhood solutions, all the variables are modified, and the magnitude of modification is governed by the normal distribution of probability.
- The neighborhood solution in the direction that has been rejected at the previous step is automatically rejected to reduce the computational cost for function evaluation.
- Local search is conducted several times at the same temperature level.
- A sharing function approach developed for genetic algorithms [21] is used to maintain diversity of the Pareto solutions.

TS, which is originally developed for single objective problem [14], has also been proven to be effective to MOP [22]. In TS, the best solution in the neighborhood is selected as the next candidate, and a tabu list is used to prevent a local cyclic search among small number of solutions. We modify the approach in [23] as

- The best solution in the candidate list is selected as the seed solution for the next step; whereas it was randomly selected in the original algorithm.
- A sharing function and niche count are used for modification of the performance function of a solution.

5 Numerical results

5.1 Analysis Model

Pareto solutions are found for a 5-story 4-span plane frame as shown in Fig. 1. Only the mass of the slab is included in the story mass that does not depend on the sizes of the columns and beams. The vertical load due to the story mass is applied at each

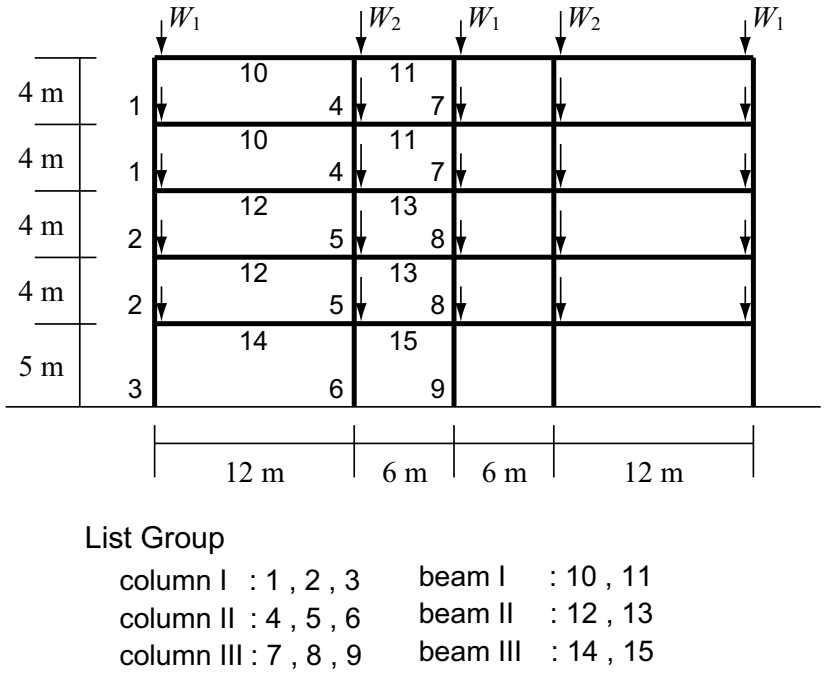

Fig. 1: A 5 story 4 span planar frame model.

beam-to-column connection before conducting time-history analysis, where $W_1 = 245$ kN and $W_2 = 343$ kN. The following two kinds of groups are utilized for definition of the design variables:

Member Group: Symmetrically located members have the same section.

List Group: The sections of the vertically aligned columns and the beams in the same floor, respectively, are selected from the same lists.

The numbers $1, 2, 3, ...$ in Fig. 1 denote the Member Groups. The List Groups are shown below the frame in Fig. 1; e.g., the members in Member Groups 1, 2 and 3 are selected from the same list. Table 1 shows the size of the sections of the members in each List Group. The standard sections in each list are shown in Tables 2 and 3 for columns and beams, respectively.

The average drift ratio β for the definition (1) of the collapse state is 0.02. Note that any larger value can be used for β, if necessary. The initial value of PGV in (2) is $v_1^{\max} = 0.5$ m/s, which is equal to the level of the severe earthquake motion for inelastic design that is traditionally used in Japan. The increment is given as $\Delta v^{\max} = 0.05$ m/s. The upper bound $\bar{R}^{\max}$ for the interstory drift ratio for $v_1^{\max} = 0.5$ m/s is 1/75, which is slightly larger than the upper bound 1/100 adopted in Japan to allow more variety of designs in the framework of performance-based design. Time-history analysis is carried out by CLAP [24], where the P-Δ effect is considered, and the material nonlinearity is modeled by the generalized plastic hinge. Young's modulus is $E = 205.8$ kN/mm^2, Poisson's ratio is 0.3, and the yield stress is 265 kN/mm^2. The bilinear stress-strain relation with kinematic hardening is used, where the stiffness after yielding is $0.01E$. The duration of each seismic motion is taken

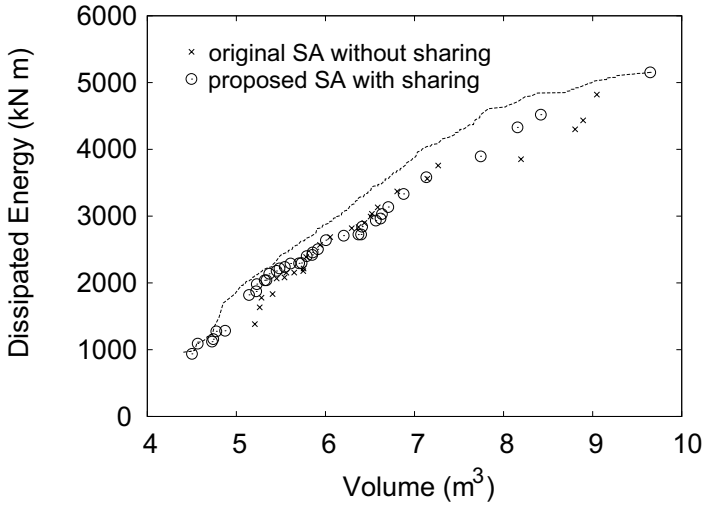

Fig. 2: Comparison of solutions obtained by original and proposed SAs with 3000 analyses. Dotted line: Pareto front by 30000 analyses.

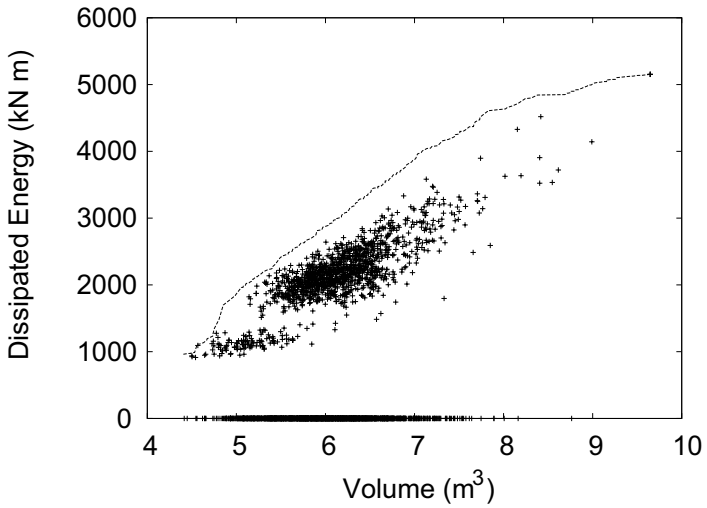

Fig. 3: All solutions generated by proposed SA with 3000 analysis. Dotted line: Pareto front by 30000 analyses.

as 10 sec., because the maximum response occurs within 10 sec. for all of the three motions. The stiffness-proportional damping is used, where the damping ratio for the fundamental mode is 0.02.

5.2 Pareto Optimal Solutions in the Objective Space.

The Pareto solutions found by the proposed SA with sharing function is shown by ∘ in Fig. 2 in the space of the objective functions. Three sets of optimization process with 1000 analyses from different initial solutions are combined to find Pareto solution with

3000 analyses, because no significant improvement of solutions has been observed after 1000 analyses for each set. The Pareto front obtained by 30000 preliminary analyses, which is regarded as an accurate set of the Pareto solutions, is plotted by the dotted line. The $\times$ marks in Fig. 2 are the Pareto solutions found by three sets of 1000 analyses by the original SA without sharing function. Note that only the effect of the use of sharing function is investigated, because it is the most effective option for both of SA and TS. The range of the solutions and the number of Pareto solutions obtained by the original and proposed SAs are shown in Table 4. The number of Pareto solutions obtained by proposed SA that dominate those by the original SA, or vice versa, which are called superior solutions for simplicity, are also listed in Table 4. The range of the Pareto front by 30000 analysis is shown in the last row of Table 4. It is seen from these results that more solutions distributed in wider range can be found by incorporating sharing function. The increase of the number of superior solutions also indicates improvement of accuracy of the solutions.

Fig. 3 shows all the solutions generated in the process of SA with 3000 analyses. Note that the solutions with $E_{\mathrm{p}}^{\max} = 0$ located along the abscissa do not satisfy the constraint (7) on the maximum interstory drift ratio at the first analysis with $k = 1$, where the PGV is equal to 0.5 m/s. These solutions are unconditionally rejected without further carrying out incremental dynamic analysis. Thus the total computational cost can be reduced by utilizing the constraint (7) on the interstory drift ratio. The ratio of the number of these rejected solutions to the number of total solutions is 44.2%; i.e., almost half of the solutions are infeasible. As can be seen from Fig. 3, SA searches a wide range in the objective space, but cannot reach the Pareto front. This is a general property of SA that has been observed in the results with different initial solutions.

The two sets of Pareto solutions found by the proposed TS with 3000 analyses called TS3000-1 and TS3000-2 are shown in Fig. 4, where the Pareto front obtained by 30000 preliminary analyses is also plotted. Fig. 5 shows all the solutions generated by TS3000-1. As can be seen, TS searches the solutions near the Pareto front.

It is seen from Figs. 2 and 4 that the TS has more accuracy than SA, and has good diversity if the results of the two sets of 3000 analyses are combined. However, the search space of TS depends on the initial solution as observed in Fig. 4, where the region with larger V and $E_{\mathrm{p}}^{\max}$ are searched by TS3000-1 and the remaining region is searched by TS3000-2. The ratios of the numbers of the rejected solutions along the abscissa of Fig. 5 to the number of total solutions is 16.7% which is much smaller than that of SA. Therefore, TS has the advantage in searching the space of the feasible solutions.

The results by the proposed TS is compared in Fig. 6 with those of the original TS without sharing function. Although no drastic increase is observed in the range and number of solutions, the number of the superior solutions by the proposed TS is more than three times of that by the original TS. Therefore, the accuracy of the Pareto solutions is improved by incorporating the sharing function.

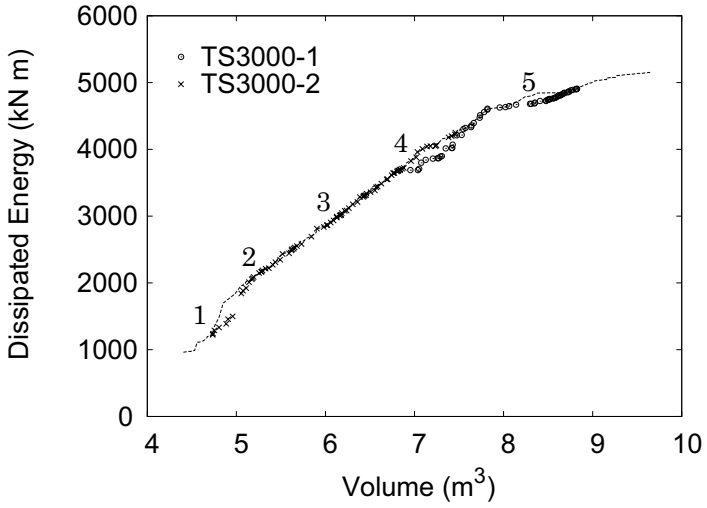

Fig. 4: Two sets of Pareto solutions obtained by proposed TS with 3000 analyses. Dotted line: Pareto front by 30000 analyses.

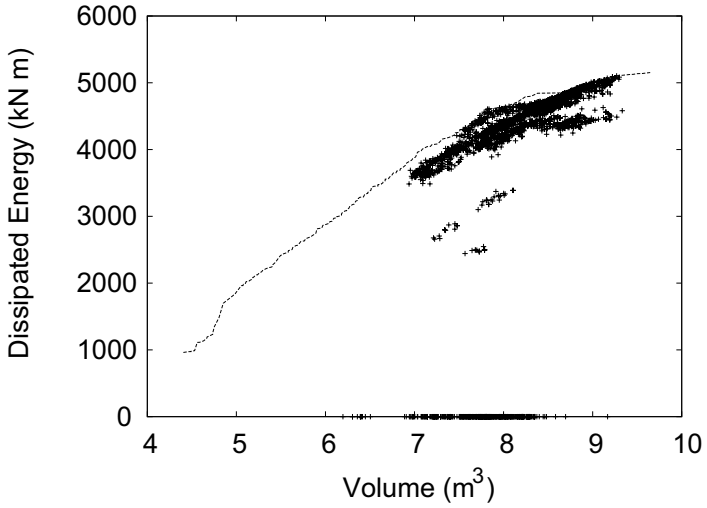

Fig. 5: All solutions generated by TS3000-1. Dotted line: Pareto front by 30000 analyses.

5.3 Properties of the Pareto Optimal Solutions.

The properties of the Pareto solutions are discussed based on the results of TS3000-2. Fig. 7 shows the relation between the objective functions V and $E_{\mathrm{p}}^{\max}$ of the Pareto solutions. Each mark distinguishes the PGV at the collapse state, which increases as V is increased. Even for the frames that collapse under the seismic motions of the same PGV, $E_{\mathrm{p}}^{\max}$ is an increasing function of V so as to form the smooth Pareto front. A design with widely distributed plastic hinges can be obtained by selecting a solution from the set of Pareto solutions. Thus, the most preferred solutions for various levels of PGV at collapse can be obtained.

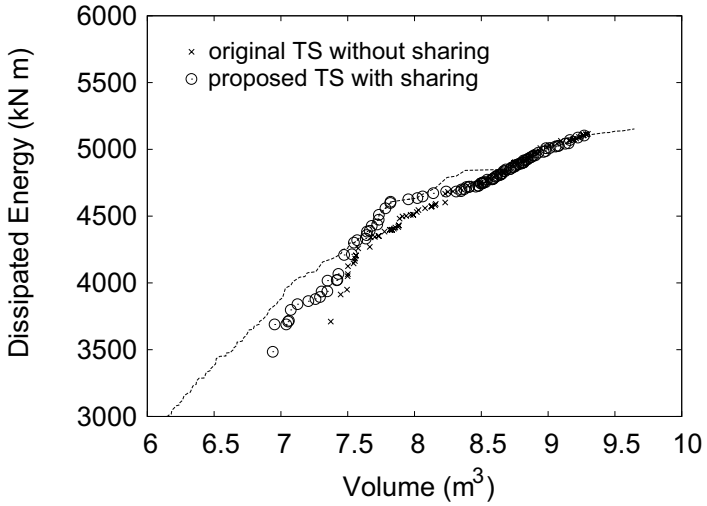

Fig. 6: Comparison of the solutions by original and proposed TSs with 3000 analyses; close view in the larger region of the objective functions of TS3000-1.

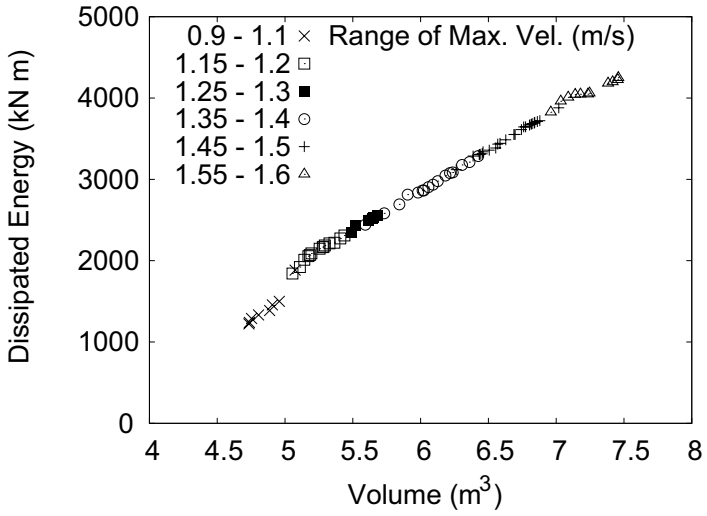

Fig. 7: Maximum velocity of seismic motion leading to collapse state of the Pareto solutions.

The characteristics of the Pareto solutions are investigated for the solutions that collapse under seismic motions with $v_k^{\max} = 1.2\,\mathrm{m/s}$. The typical designs named Solutions 1–5 are selected as indicated in Fig. 4. The cross-sectional areas of Solution 3 are as shown in Fig. 8, where the width of each member is proportional to its cross-sectional area. It can be observed from Fig. 8 that Solution 3 has large sections for internal beams and columns, which is a general property of the Pareto solutions as seen in Fig. 9.

The total volume, dissipated energy and the story drift ratios of Solutions 1–5 are listed in Table 5. It is seen that the The lower 3 stories have almost the same maximum drift ratios; i.e. the frames collapse uniformly.

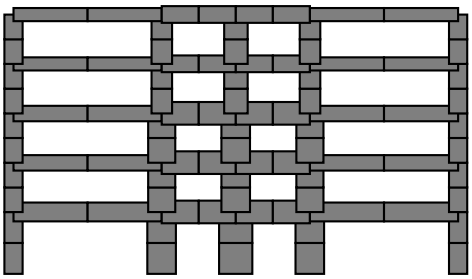

Fig. 8: Cross-sectional areas of Solution 3.

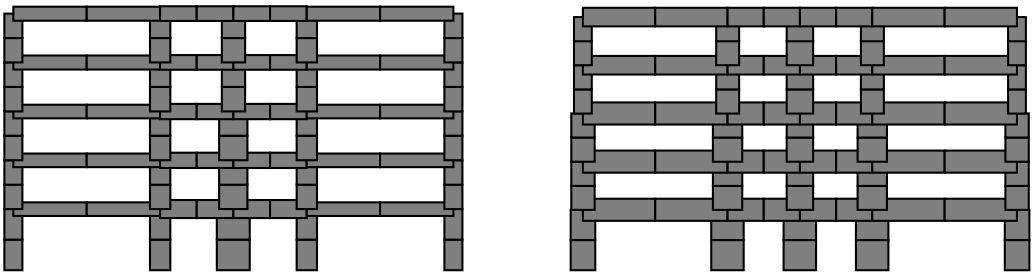

(a) Solution 1 (b) Solution 5

Fig. 9: Cross-sectional areas of Solutions 1 and 5.

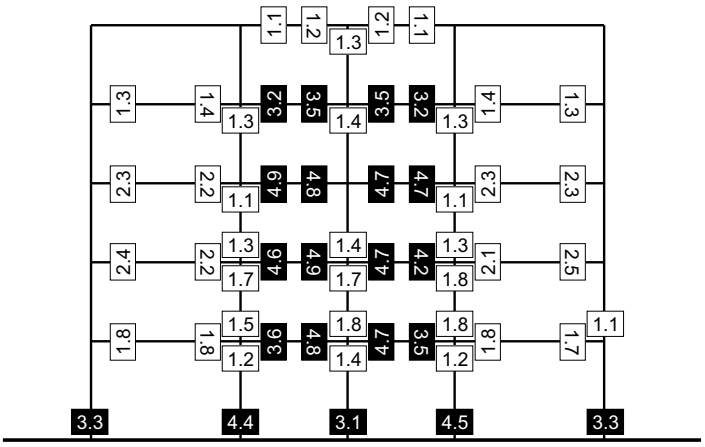

Fig. 10: Ductility ratios of Solution 3.

Fig. 10 shows the maximum ductility ratios of the plastic hinges at the ends of each member of Solution 3. The member ends without the values in Fig. 10 remain elastic at the collapse state. The ductility ratios greater than 3.0 are written in a white number in a black box. Note that large plastic deformation exists in the column base and the internal beams, and no large deformation can be found in the columns except at the base. This way, the Pareto solutions with favorable uniform story collapse can be generated by solving the multiobjective optimization problem, and many alternative designs can be simultaneously obtained.

6 Conclusions

An MOP problem has been formulated to simultaneously minimize the total structural volume and maximize the plastic dissipated energy at the collapse state. Incremental dynamic analysis is carried out to determine the PGV of the seismic motion that leads to the collapse state. The design variables are cross-sectional properties that are selected from the list of the standard sections. SA and TS have been used to obtain the set of Pareto solutions. The conclusions obtained from this study are summarized as follows:

- A frame that collapses with a uniform interstory drift ratio can be obtained as a Pareto solution that simultaneously minimize the structural volume and maximize the dissipated energy at collapse state. Many alternative designs or compromise solutions can be obtained as a set of Pareto solutions.
- The optimal cross-sections, which are to be selected from the list of available standard sections, can be found by solving a combinatorial optimization problem.
- SA and TS can be successfully used for a multiobjective structural optimization problem that demands large computational cost for the function evaluation. However, TS is an advantage over SA in view of the diversity of the Pareto solutions and the ability of searching the solutions near the Pareto front.
- The accuracy and diversity of the Pareto solutions by SA and TS can be improved by using sharing functions that are used in multiobjective genetic algorithm.

7 Acknowledgement

The authors are grateful to Prof. M. Tada of Osaka University of Japan for kindly offering "CLAP" source code.

References

[1] A. Whittaker, M. Constantinou, and P. Tsopelas. Displacement estimates for performance-based seismic design. *J. Struct. Eng., ASCE*, 124(8):905–912, 1998.

[2] Q. Xue and C.C. Chen. Performance-based seismic design of structures: a direct displacement-based approach. *Engineering Structures*, 25:1803–1813, 2003.

[3] R. Hasan, L. Xu, and D.E. Grierson. Push-over analysis for performance-based seismic design. *Comp. & Struct.*, 80:2483–2493, 2002.

[4] R. J. Balling, K. S. Pister, and V. Ciampi. Optimal seismic-resistant design of a planar steel frame. *Earthquake Eng. Struct. Dyn.*, 11:541–556, 1983.

[5] S. Mahin, J. Malley, and R. Hamburger. Overview of the FEMA/SAC program for reduction of earthquake hazards in steel moment frame structures. *J. Constructional Steel Research*, 58:511–528, 2002.

[6] S. Leelataviwat, S. C. Goel, and B. Stojadinović. Energy-based seismic design of structures using yield mechanism and target drift. *J. Struct. Eng., ASCE*, 128(8):1046–1054, 2002.

[7] X.-K. Zou and C.-M. Chan. An optimal resizing technique for seismic drift design of concrete buildings subjected to response spectrum and time history loadings. *Comp. & Struct.*, 83:1689–1704, 2005.

[8] S. Burns, editor. *Recent advancements in optimal structural design.* ASCE, 2002.

[9] R. T. Haftka, Z. Gürdal, and M. P. Kamat. *Elements of Structural Optimization.* Kluwer Academic Publishers, 1990.

[10] M.-W. Huang and J. S. Arora. Optimal design of steel structures using standard sections. *Struct. Multidisc. Optim.*, 14:24–35, 1997.

[11] C. Reeves. *Modern Heuristic Techniques for Combinatorial Problems.* McGraw-Hill, New York, 1995.

[12] D. E. Goldberg. *Genetic Algorithms in Search, Optimization, and Machine Learning.* Addison-Wesley, Reading, MA, 1989.

[13] E. Aarts and J. Korst. *Simulated Annealing and Boltzmann Machines: A Stochastic Approach to Combinatorial Optimization and Neural Computing.* Wiley, Chichester, England, 1989.

[14] F. Glover. Tabu search – part I. *ORSA J. on Computing*, 1:190–206, 1989.

[15] M. Liu, S. A. Burns, and Y. K. Wen. Multiobjective optimization for performance-based seismic design of steel moment frame structures. *Earthquake Eng. Struct. Dyn.*, 34(3):289–306, 2004.

[16] T. Marler and J. S. Arora. Survey of multi-objective optimization methods for engineering. *Struct. Multidisc. Optim.*, 26(6):369–395, 2004.

[17] R. O. Hamburger, D. A. Foutch, and C. A. Cornell. Performance basis of guidelines for evaluation, upgrade and design of moment-resisting steel frames. In *Proc. 12th World Congress of Earthquake Eng.*, page Paper No. 2543, 2000.

[18] J. L. Cohon. *Multiobjective Programming and Planning*, volume 140 of *Mathematics in Science and Engineering.* Academic Press, 1978.

[19] J. F. Whidborne, D. W. Gu, and I. Postlethwaite. Simulated annealing for multi-objective control system design. *IEE Proc. Control Theory Appl.*, 144(6):582–588, 1997.

[20] C. D. Jilla and D. W. Miller. Assessing the performance of a heuristic simulated annealing algorithm for the design of distributed satellite systems. *Acta Astronautica*, 48(5):529–543, 2001.

[21] D. E. Goldberg and J. Richardson. Genetic algorithms with sharing for multimodal function optimization. In *Proc. 2nd Int. Conf. Genetic Algorithms*, 1987.

[22] M. P. Hansen. Tabu search for multiobjective optimization: Mots. In *Proc. 13th Int. Conf. on MCDM*, pages 6–10, Cape Town, 1997.

[23] A. Baykasoglu, S. Owen, and N. Gindy. A taboo search based approach to find the pareto optimal set in multiple objective optimization. *Eng. Opt.*, 31:731–748, 1999.

[24] K. Ogawa and M. Tada. Computer program for static and dynamic analysis of steel frames considering the deformation of joint panel. In *Proc. 17th Symp. on Comp. Tech. of Information, Sys. and Appl.*, pages 79–84, 1994. (in Japanese).

Table 1: Size of the sections of the members in each List Group.

column I	□-400 series
column II	□-500 series
column III	□-500 series
beam I	H-500 series
beam II	H-600 series
beam III	H-600 series

Table 2: Column sections.

□ - 400 series

J_i	size (mm)	A^i ($\times 10^4$ mm^2)	I^i ($\times 10^8$ mm^4)	$Z^i_{\rm p}$ ($\times 10^6$ mm^3)
1	$\square - 400 \times 12$	1.788	4.38	2.56
2	$\square - 400 \times 16$	2.326	5.52	3.28
3	$\square - 400 \times 19$	2.710	6.28	3.77
4	$\square - 400 \times 22$	3.077	6.95	4.22
5	$\square - 400 \times 25$	3.428	7.54	4.64

□ - 500 series

J_i	size (mm)	A^i ($\times 10^4$ mm^2)	I^i ($\times 10^8$ mm^4)	$Z^i_{\rm p}$ ($\times 10^6$ mm^3)
1	$\square - 500 \times 12$	2.268	8.84	4.10
2	$\square - 500 \times 16$	2.966	11.30	5.29
3	$\square - 500 \times 19$	3.470	13.00	6.13
4	$\square - 500 \times 22$	3.957	14.50	6.92
5	$\square - 500 \times 25$	4.428	15.90	7.66
6	$\square - 500 \times 28$	4.883	17.20	8.36
7	$\square - 500 \times 32$	5.463	18.70	9.21
8	$\square - 500 \times 36$	6.014	20.00	9.97

Table 3: Beam sections.

H - 500 series				
J_i	size (mm)	A^i ($\times 10^4$ mm^2)	I^i ($\times 10^8$ mm^4)	Z_{p}^i ($\times 10^6$ mm^3)
1	H $-$ 500 $\times$ 200 $\times$ 9 $\times$ 12	0.923	3.75	1.72
2	H $-$ 500 $\times$ 200 $\times$ 9 $\times$ 16	1.076	4.60	2.08
3	H $-$ 500 $\times$ 200 $\times$ 9 $\times$ 19	1.190	5.21	2.34
4	H $-$ 500 $\times$ 200 $\times$ 9 $\times$ 22	1.305	5.81	2.60
5	H $-$ 500 $\times$ 200 $\times$ 12 $\times$ 22	1.442	6.05	2.76
6	H $-$ 500 $\times$ 250 $\times$ 9 $\times$ 22	1.525	7.07	3.13
7	H $-$ 500 $\times$ 250 $\times$ 12 $\times$ 22	1.662	7.31	3.29
8	H $-$ 500 $\times$ 250 $\times$ 12 $\times$ 25	1.804	8.04	3.61
9	H $-$ 500 $\times$ 250 $\times$ 12 $\times$ 25	1.947	8.75	3.93
H - 600 series				
J_i	size (mm)	A^i ($\times 10^4$ mm^2)	I^i ($\times 10^8$ mm^4)	Z_{p}^i ($\times 10^6$ mm^3)
1	H $-$ 600 $\times$ 200 $\times$ 9 $\times$ 12	1.013	5.70	2.20
2	H $-$ 600 $\times$ 200 $\times$ 9 $\times$ 19	1.280	7.86	2.96
3	H $-$ 600 $\times$ 200 $\times$ 12 $\times$ 22	1.562	9.18	3.51
4	H $-$ 600 $\times$ 250 $\times$ 12 $\times$ 22	1.782	11.00	4.15
5	H $-$ 600 $\times$ 250 $\times$ 12 $\times$ 25	1.924	12.10	4.54
6	H $-$ 600 $\times$ 250 $\times$ 16 $\times$ 28	2.285	13.70	5.23
7	H $-$ 600 $\times$ 300 $\times$ 12 $\times$ 28	2.347	15.50	5.73
8	H $-$ 600 $\times$ 300 $\times$ 16 $\times$ 28	2.565	16.00	6.03
9	H $-$ 600 $\times$ 300 $\times$ 16 $\times$ 32	2.792	17.70	6.64

Table 4: Comparison of the results by the proposed SA and TS to the original methods without sharing functions.

	Volume [m^3]		Dissipated Energy [kN]		No. of	No. of
	Min.	Max.	Min.	Max.	solutions	superior solutions
SA (original)	5.21	9.05	1382.07	4819.92	26	12
SA (proposed)	4.50	9.65	937.45	5153.14	37	31
TS (original)	7.37	9.36	3710.52	5153.14	101	21
TS (proposed)	6.94	9.27	3484.76	5103.31	103	74
Pareto Front	4.40	9.65	961.75	5153.14	-	-

Table 5: Total volume, dissipated energy and interstory drifts of Solutions 1–5.

Solution	Volume (m^3)	Dissipated Energy ($kN \cdot m$)	Story Drift Ratio ($\times 10^{-2}$)				
			1	2	3	4	5
1	4.715	1269.9	3.6160	2.8926	2.7763	2.4588	1.2720
2	5.328	2212.7	3.2760	2.6208	2.6657	2.0847	1.5753
3	6.127	2993.1	3.4085	2.7268	2.8153	2.4748	1.8625
4	7.013	3889.6	3.6018	2.8814	2.4655	2.4818	1.8150
5	8.330	4770.3	3.9145	3.1316	2.5125	2.0860	1.3488